ChemComm

COMMUNICATION

View Article Online
View Journal

Cite this: DOI: 10.1039/d5cc03785a

Received 4th July 2025,
Accepted 9th September 2025

DOI: 10.1039/d5cc03785a

rsc.li/chemcomm

Bleaching effect of high refractive index xylylic poly(thiourea)s with "de-conjugated" polarizable hydrogen bonds

Seigo Watanabe, [a] Yoshino Tsunekawa[b] and Kenichi Oyaizu *[ab]

Poly(*p*-xylylene thiourea) (*p*X-PTU) exhibits high visible-light transparency (%*T* ≧ 99), a high refractive index (n_D = 1.71), and a reasonable Abbe number (ν_D = 26) owing to "de-conjugated" hydrogen bonds, which inhibit orbital interactions between the polarizable phenylene and thiourea units through sandwiched methylene spacers. Upon blending *p*X-PTU with all-aromatic poly(thiourea)s, their refractive index increased up to n_D = 1.80.

High refractive index polymers (HRIPs) typically exhibit refractive indices (RI) above 1.7 and are essential in various optoelectronic applications, including lighting devices, waveguides, and augmented/mixed reality (AR/MR).[1–5] To date, numerous HRIPs have been developed based on the Lorentz–Lorenz equation, which requires optimizing high polarizability and small molecular volume to achieve the desired RI and transparency at the target wavelength.[2,4] The most common HRIP categories are sulfur-containing polymers, such as poly(phenylene sulfide)s,[4,6–10] sulfur-rich polymers,[3,11–13] and thioacetal-containing polymers.[14,15] In particular, HRIPs with excessive sulfur content or conjugated π-skeletons achieve ultrahigh RI (over 1.8),[11,16,17] but they are colored due to the orbital interactions among π-skeletons and/or sulfur lone pairs (*e.g.*, n–π interactions[18]). To address this empirical dilemma, we previously developed hydrogen-bonding (H-bonding) poly(phenylene sulfide)s to achieve both ultrahigh RI (n_D ∼ 1.80–1.85) and visible-light transparency.[19,20] The key factor lies in the reduced free volume, which enhances the RI without compromising UV-visible (UV-vis) transparency. We further extended this concept to all-aromatic poly(thiourea)s (PTUs) featuring multiple and polarizable H-bonds, exhibiting better RI (n_D ∼ 1.7–1.8) and flexibility owing to strengthened PTU networks.[21,22] Also, other researchers have recently reported diverse high-RI PTU structures.[23,24] However, although all-aromatic PTU thin films are nearly colorless, their transparency remains low (%T ≥ 92, 1 μm thick) owing to the direct coupling of polarizable thiourea and aromatic rings, which leads to excessive orbital interactions resulting in near-UV absorption and small Abbe numbers (ν_D = 11–18).[21]

In this study, we provide a new concept, termed as "de-conjugated" polarizable H-bonds, to significantly enhance the transparency of high-RI PTUs (Fig. 1). The key design is poly(xylylene thiourea) (X-PTU), which contains a sandwiched methylene spacer that separates polarizable aromatic and thiourea groups, thereby inhibiting orbital interactions. In particular, *p*-substituted X-PTU (***p*X-PTU**) exhibited amorphous and thermal properties comparable to those of the all-aromatic PTUs, while displaying improved transparency (%T ≥ 99) and a higher Abbe number (ν_D = 26) with its high RI (n_D = 1.71) maintained (Fig. 1, right). In addition, ***p*X-PTU** showed good miscibility with all-aromatic poly(1,3-phenylene-*alt*-1,4-phenylene thiourea) (***mp*Ph-PTU**), producing simply blended transparent films with an enhanced T_g and well-balanced optical properties (T_g = 164 °C, n_D = 1.80, ν_D = 17). Overall, this study highlights the potential of the "de-conjugated" H-bonding X-PTU and its polymer blends as a rational approach to simultaneously maximize various properties (*e.g.*, RI, Abbe numbers, and transparency) for versatile optoelectronic polymers.

The X-PTUs were synthesized following our previous report,[21] involving the polycondensation of xylylene diamines (XDA) and 1,1-thiocarbonyl diimidazole (Schemes S1 and S2).

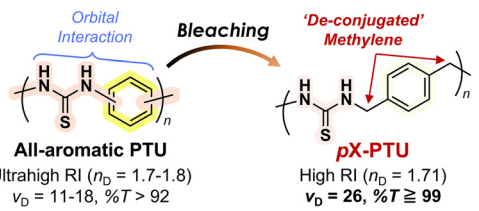

Fig. 1 The concept of "de-conjugated" polarizable H-bonds: from all-aromatic PTU[21] (left: prior work) to ***p*X-PTU** (right: this work) to bleach high-RI PTUs.

[a] *Research Institute for Science and Engineering, Waseda University, 3-4-1 Okubo, Shinjuku-ku, Tokyo 169-8555, Japan. E-mail: oyaizu@waseda.jp*
[b] *Department of Applied Chemistry, Waseda University, 3-4-1 Okubo, Shinjuku-ku, Tokyo 169-8555, Japan*

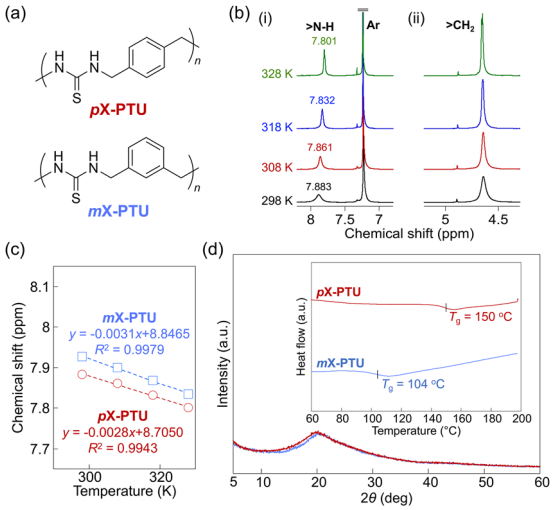

Fig. 2 Properties of X-PTUs. (a) Chemical structures of ***p*X-PTU** and ***m*X-PTU**. (b) ^{1}H VT-NMR of ***p*X-PTU** (i) at 8.2–6.8 ppm (>N–H and aromatic signals) and (ii) at 5.2–4.3 ppm (methylene signals). (c) Temperature dependence of >N–H chemical shifts in ^{1}H VT-NMR. (d) XRD profiles (inset: DSC thermograms at a scan rate of 20 °C min^{-1}).

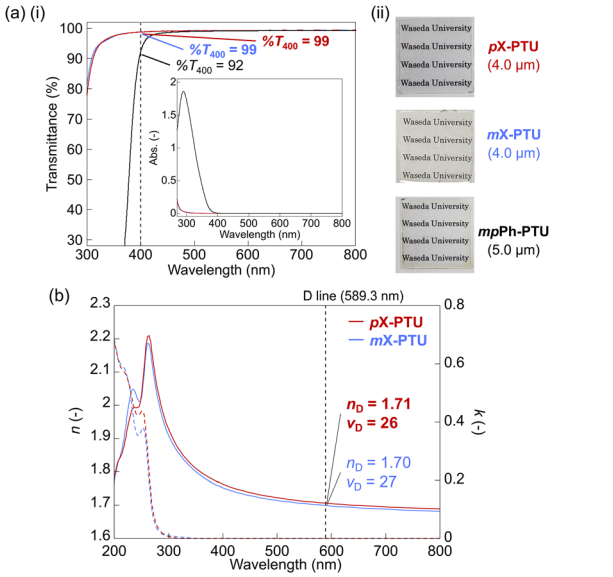

Fig. 3 Optical properties of X-PTUs. (a) (i) Normalized UV-vis spectra for the films (thickness: 1 μm) of X-PTUs and ***mp*Ph-PTU** (inset: UV-vis absorbance spectra of 0.1 mM solution in DMF). (ii) Photographs of PTU thin films on glass substrates and their thickness. (b) RI spectra: *n* (solid line) and *k* (dotted line).

Two *m*- and *p*-substituted PTU isomers (***m*X-PTU** and ***p*X-PTU**) were obtained as high-molecular-weight polymers ($M_w \sim 10^5$), owing to the higher nucleophilicity of XDAs compared with that of all-aromatic diamines (Fig. 2a). The resulting X-PTUs were characterized by ^{1}H and ^{13}C NMR spectroscopy, showing signals of thiourea, aromatic, and methylene groups (Fig. S1–S4). The IR spectra indicate two N–H conformations of thiourea ($\nu_{N-H(trans/trans)}$: ~3270 cm^{-1} and $2\delta_{N-H(cis/trans)}$: ~3055 cm^{-1}), suggesting the presence of randomized H-bond networks (Fig. S5). Upon increasing the temperature, the ^{1}H variable-temperature (VT) NMR spectra of the X-PTUs showed an upfield shift exclusively for the H-bonding amino signals (7.93–7.80 ppm) (Fig. 2b and Fig. S6). Notably, ***p*X-PTU** exhibited lower temperature dependence (-2.8×10^{-3} ppm K^{-1}) than ***m*X-PTU** (-3.1×10^{-3} ppm K^{-1}) and previously reported phenylene-PTUs ($< -3.5 \times 10^{-3}$ ppm K^{-1})[21] (Fig. 2c). These results indicate that ***p*X-PTU** contains stronger and more high-temperature-resistant intermolecular H-bond network.

Regarding the crystalline properties, the X-ray diffraction (XRD) profiles indicate an amorphous nature of X-PTUs, which can be attributed to the zig-zag H-bonds of the thiourea arrays (Fig. 2d). **X-PTU** exhibited good thermostability, with both an adequate T_g (>100 °C) and a high pyrolysis temperature (T_{d5} ~ 240–250 °C), significantly surpassing those of phenylene-PTUs (T_g ~ 150 °C, T_{d5} ~ 180 °C)[21] (Fig. 2d inset, Fig. S7). This superior thermostability can be attributed to the deconjugated X-PTU structure containing methylene spacers, which enhance the bond stability (dissociation energy) of the C–N bonds, similar to the effect observed in aromatic/xylylic poly(dithiourethane)s.[25] Among the X-PTUs, ***p*X-PTU** showed a significantly higher T_g (150 °C) than ***m*X-PTU** (T_g = 104 °C), owing to the stronger and more temperature-resistant interchain H-bonds in the linear-shaped *p*-phenylene skeleton compared with the bent-shaped *m*-phenylene unit.

Their optical properties were investigated to confirm the introduction effect of "de-conjugated" H-bonds (Fig. 3). The solution UV-vis spectra displayed that the X-PTUs exhibit superior visible-light transparency compared with ***mp*Ph-PTU**, accompanied by a blue shift in near-UV absorption (Fig. 3a inset). This behavior can be attributed to the absence of orbital interactions between the lone pairs/π-electrons of the thioureas and phenylene rings upon the introduction of methylene spacers. To gain molecular-level insight, density functional theory (DFT) calculations were conducted on the model compounds of each polymer (Fig. S8). The orbital geometries of the phenylene-PTU models exhibited a widely distributed highest occupied molecular orbital (HOMO), which strongly overlapped with the lowest unoccupied molecular orbital (LUMO). In contrast, the X-PTU model showed a narrower distribution of continuous HOMO orbitals and less HOMO–LUMO geometry overlap. The estimated UV-vis spectra by time-dependent (TD) DFT calculations reproduced a pronounced blue shift in the near-UV absorption for the X-PTU models (Fig. S9). Therefore, the effect of "de-conjugated" methylene spacers in X-PTUs can be rationalized as the suppression of orbital interactions between thioureas and phenylene rings.

X-PTU thin films were also prepared *via* drop-casting or spin-coating, exhibiting colorless and visually transparent features (Fig. 3a), and the ***p*X-PTU** film displayed a fluorescence emission under UV irradiation (Fig. S10), as observed in typical PTUs.[26] Their UV-vis spectra display higher near-UV-vis transparency (%$T \geq 99$) than those of aromatic PTUs, owing to the bleaching effect in the X-PTUs (Fig. 3a(i) and Fig. S11). Following the introduction of methylene spacers, the X-PTUs exhibited lower RI (n_D = 1.71 (***p*X-PTU**) and 1.70 (***m*X-PTU**)) than previously reported phenylene-PTUs (n_D ~ 1.8)[21] because of the

decrease in the unit polarizability (Fig. 3b). However, their RI remained within the range of typical HRIPs,[2,4] while the Abbe numbers were markedly improved (ν_D = 26 (***p*X-PTU**) and 27 (***m*X-PTU**)) compared with those of the reported phenylene-PTUs (ν_D ~ 11–15)[21] and dimethyl-substituted PPS with a similar RI (n_D = 1.69, ν_D = 18).[27] These trends follow the classical Kramers–Kronig relationship,[28] which explains that suppressing the near-UV absorption in X-PTUs results in a higher ν_D. Furthermore, despite the low UV stability of aromatic PTUs ascribed to the presence of reactive C=S bonds[29] that induced lower transparency and RI (Fig. S12 and S13), the optical properties of ***p*X-PTU** were less deteriorated after the UV treatment than those for ***mp*Ph-PTU**, thanks to the "de-conjugated" xylylene unit with less orbital interactions. In addition, there has been minimal change in RI and transparency of ***p*X-PTU** after the high-temperature or humid exposure (difference of $\%T_{400}$ ~ 1%, n_D ~ ±0.01) (Fig. S14–S17), attributed to the high hydrophobicity and rigidity (T_g) of the aromatic main chain and the relatively hydrophobic H-bond properties[30] of the thiourea moieties to prevent H-bond network destruction. Finally, the ***p*X-PTU** film displayed higher stress (17.2 MPa) and smaller strain (0.64%) upon fracture than the previous aromatic PTU (12 MPa, 2.4%)[22] (Fig. S18), suggesting higher mechanical robustness due to the stronger H-bond nature of X-PTUs (Fig. 2c: *vide supra*).

In light of the high-RI yet transparent optical properties of X-PTU, we further adjusted the thermostability and RI while maintaining high transparency by applying a blending strategy with different PTUs.[31] We selected ***mp*Ph-PTU** as a blending counterpart because of its higher T_g (175 °C) and RI (n_D = 1.81). Each PTU was blended by precipitating the DMF solution into methanol, yielding ***p*X-PTU**/***mp*Ph-PTU** blends with ***p*X-PTU** molar ratios of $x_{pX\text{-}PTU}$ = 0.72, 0.49, and 0.24 (Fig. S19–S21). Their DSC thermograms display a single T_g that shifts to higher temperature as $x_{pX\text{-}PTU}$ decreases (Fig. 4a), indicating good miscibility between each PTU with 10–20 nm scale homogeneity.[32] To further elucidate their miscibility on a smaller scale, we conducted cross-polarization/magic angle spinning (CP/MAS) ^{13}C NMR on the ***p*X-PTU**/***mp*Ph-PTU** blends (Fig. S23–S27). In short, the ^{1}H spin–lattice relaxation time ($T_{1\rho}$) was determined from two areas, aromatic (*ca.* 150–100 ppm) and methylene (*ca.* 55–35 ppm) signals, for each composition (Fig. S28). While those $T_{1\rho}$s did not match perfectly, they shifted proportionally with $x_{pX\text{-}PTU}$, confirming interdomain interactions between ***p*X-PTU** and ***mp*Ph-PTU** in the blended matrices (Fig. 4b and Table S1). Therefore, although those PTUs were phase-separated on a 3–4 nm scale detectable by CP/MAS NMR measurements, they are miscible on a scale below 20 nm, as indicated by the T_g shifts observed in the DSC results.

The drop-cast ***p*X-PTU**/***mp*Ph-PTU** blend films were visibly transparent and exhibited no aggregation, further confirming the good miscibility of the PTUs (Fig. 5a inset). The UV-vis spectra of the blend films showed good transparency (94–96%T for 1 μm thickness), falling between the values of the individual PTUs regardless of the film thickness (Fig. 5a, Table S2, and Fig. S29–S31). These results demonstrated the bleaching effect with improved near-UV transparency upon increasing $x_{pX\text{-}PTU}$. Their ATR-IR spectra showed a consistent peak shift of the H-bonded N–H vibration modes (ν_{N-H} and $2\delta_{N-H}$) (Fig. S32), indicating the presence of homogeneous H-bond networks even in the blended states without any macroscopic phase separation.

The RI spectra also followed consistent shifts in n_D and ν_D corresponding to the blending ratio (Fig. 5b). In short, the ***p*X-PTU**/***mp*Ph-PTU** blend with higher $x_{pX\text{-}PTU}$ exhibited a lower RI and higher ν_D across the entire visible-light region, aligning well with the empirical RI–Abbe trade-off relationship[33] (Fig. 5c). The extinction coefficient (k, the imaginary part of the complex RI) also decreased with higher $x_{pX\text{-}PTU}$, demonstrating the bleaching effect upon ***p*X-PTU** introduction (Fig. S33). Summarizing the above, ***p*X-PTU** was miscible with aromatic PTU on a 10–20 nm scale, and their polymer blends produced transparent films with enhanced thermostability and RI. In particular, entry 3 ($x_{pX\text{-}PTU}$ = 0.24; Table S2) showed the best balance of thermal and optical

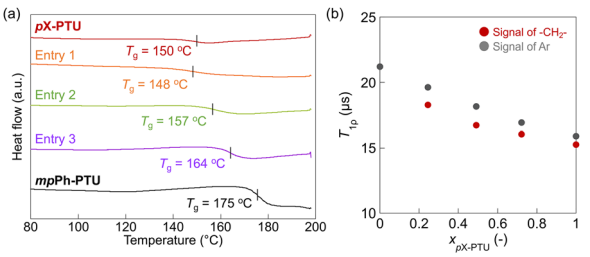

Fig. 4 Miscibility studies of ***p*X-PTU** and ***mp*Ph-PTU**. (a) DSC thermograms of the blends (2nd heating, scanning rate: 20 °C min^{-1}). (b) Relationship between ^{1}H spin–lattice relaxation time ($T_{1\rho}$) of the blends measured by solid-state CP-MAS ^{13}C NMR and the molar ratio of ***p*X-PTU** ($x_{pX\text{-}PTU}$).

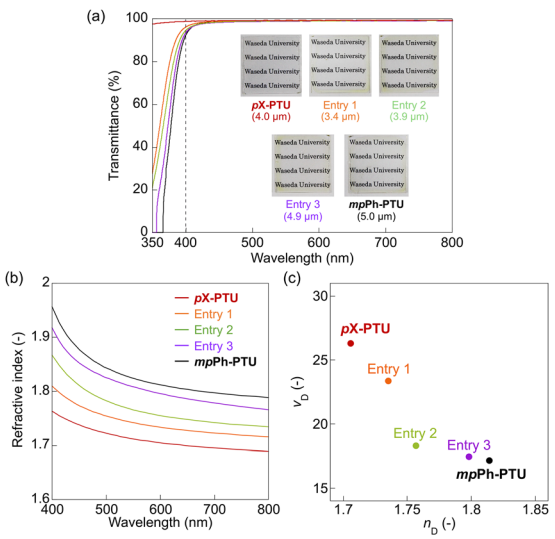

Fig. 5 Optical properties of the films of the ***p*X-PTU**/***mp*Ph-PTU** blends. (a) Normalized UV-vis spectra (film thickness: 1 μm) (inset: photographs and thickness of the films). (b) RI spectra in the visible-light region (for the overall spectra, see Fig. S32). (c) n_D *versus* ν_D.

properties among the PTU family, exhibiting a high T_g (164 °C) and ultrahigh RI (n_D = 1.80), while simultaneously achieving a reasonable Abbe number (ν_D = 17) and visible light transparency (94%T, 1 μm thickness).

In summary, we demonstrated the X-PTU family as an HRIP substructure with unprecedented near-UV-vis transparency and Abbe numbers (*e.g.*, ***p*X-PTU**: n_D = 1.71, ν_D = 26). The key molecular design lies in the "de-conjugated" H-bonds, which involves separating the polarizable aromatic and thiourea moieties with sandwiched methylene spacers to inhibit their orbital interactions while maintaining high polarizability and H-bond density. In particular, ***p*X-PTU** exhibited adequate thermostability (T_g = 150 °C) and good miscibility with ***mp*Ph-PTU** on a 10–20 nm scale, and their blended films demonstrated adjustable thermal and optical properties. To our knowledge, this study is the first to demonstrate how orbital interactions in an HRIP bearing polarizable H-bonds affect the overall optical properties. Furthermore, miscible polymer blending is verified as a simple strategy to adjust the thermal and optical properties. Expanding this concept to diverse polarizable H-bond containing HRIP skeletons (*e.g.*, poly(thioamide)s[23,34] and poly(sulfamide)s[35]) leads to the further design of optical polymers surpassing the empirical RI–Abbe trade-off limit.

This work was partially supported by Grants-in-Aid for Scientific Research (No. 21H04695, 22K18335, and 25K18083) from MEXT, Japan, the Satomi Scholarship Foundation, and ENEOS Tonen General Research/Development Encouragement and Scholarship Foundation.

Conflicts of interest

There are no conflicts to declare.

Data availability

The data supporting this article have been included as part of the SI. Supplementary information: Experimental and synthetic procedures, characterization data, computational calculation, solid-state NMR results, and additional properties for the blends. See DOI: **https://doi.org/10.1039/d5cc03785a**.

Notes and references

1 J.-G. Liu and M. Ueda, *J. Mater. Chem.*, 2009, **19**, 8907–8919.
2 T. Higashihara and M. Ueda, *Macromolecules*, 2015, **48**, 1915–1929.
3 T. S. Kleine, R. S. Glass, D. L. Lichtenberger, M. E. Mackay, K. Char, R. A. Norwood and J. Pyun, *ACS Macro Lett.*, 2020, **9**, 245–259.
4 S. Watanabe and K. Oyaizu, *Bull. Chem. Soc. Jpn.*, 2023, **96**, 1108–1128.
5 A. Nishant, K.-J. Kim, S. A. Showghi, R. Himmelhuber, T. S. Kleine, T. Lee, J. Pyun and R. A. Norwood, *Adv. Opt. Mater.*, 2022, **10**, 2200176.
6 Y. Suzuki, K. Murakami, S. Ando, T. Higashihara and M. Ueda, *J. Mater. Chem.*, 2011, **21**, 15727–15731.
7 K. Nakabayashi, T. Imai, M.-C. Fu, S. Ando, T. Higashihara and M. Ueda, *Macromolecules*, 2016, **49**, 5849–5856.
8 M.-C. Fu, Y. Murakami, M. Ueda, S. Ando and T. Higashihara, *J. Polym. Sci., Part A:Polym. Chem.*, 2018, **56**, 724–731.
9 S. Watanabe, Y. Tsunekawa, T. Takayama and K. Oyaizu, *Macromolecules*, 2024, **57**, 2897–2904.
10 S. Watanabe, Z. An, H. Nishio, Y. Tsunekawa and K. Oyaizu, *J. Mater. Chem. C*, 2025, **13**, 7933–7942.
11 J. J. Griebel, S. Namnabat, E. T. Kim, R. Himmelhuber, D. H. Moronta, W. J. Chung, A. G. Simmonds, K.-J. Kim, J. van der Laan, N. A. Nguyen, E. L. Dereniak, M. E. Mackay, K. Char, R. S. Glass, R. A. Norwood and J. Pyun, *Adv. Mater.*, 2014, **26**, 3014–3018.
12 D. H. Kim, W. Jang, K. Choi, J. S. Choi, J. Pyun, J. Lim, K. Char and S. G. Im, *Sci. Adv.*, 2020, **6**, eabb5320.
13 K.-S. Kang, C. Olikagu, T. Lee, J. Bao, J. Molineux, L. N. Holmen, K. P. Martin, K.-J. Kim, K. H. Kim, J. Bang, V. K. Kumirov, R. S. Glass, R. A. Norwood, J. T. Njardarson and J. Pyun, *J. Am. Chem. Soc.*, 2022, **144**, 23044–23052.
14 S. Watanabe, T. Yano, Z. An and K. Oyaizu, *ChemSusChem*, 2025, **18**, e202401609.
15 J.-Z. Zhao, T.-J. Yue, B.-H. Ren, Y.-X. Ma, X.-B. Lu and W.-M. Ren, *J. Am. Chem. Soc.*, 2025, **147**, 19762–19769.
16 X. Wu, J. He, R. Hu and B. Z. Tang, *J. Am. Chem. Soc.*, 2021, **143**, 15723–15731.
17 M. Lee, Y. Oh, J. Yu, S. G. Jang, H. Yeo, J.-J. Park and N.-H. You, *Nat. Commun.*, 2023, **14**, 2866.
18 A. Fukazawa, Y. Toda, M. Hayakawa, A. Sekioka, H. Ishii, T. Okamoto, J. Takeya, Y. Hijikata and S. Yamaguchi, *Chem. – Eur. J.*, 2018, **24**, 11503–11510.
19 S. Watanabe and K. Oyaizu, *Macromolecules*, 2022, **55**, 2252–2259.
20 S. Watanabe, H. Nishio, T. Takayama and K. Oyaizu, *ACS Appl. Polym. Mater.*, 2023, **5**, 2307–2311.
21 S. Watanabe, L. M. Cavinato, V. Calvi, R. van Rijn, R. D. Costa and K. Oyaizu, *Adv. Funct. Mater.*, 2024, **34**, 2404433.
22 S. Watanabe, Y. Tsunekawa and K. Oyaizu, *Macromol. Chem. Phys.*, 2025, **226**, 2400456.
23 Y. Huang, R. Hu and B. Z. Tang, *Macromolecules*, 2024, **57**, 6568–6576.
24 Y. Yu, W. Chen, R. Hu and B. Z. Tang, *Polym. Chem.*, 2025, **16**, 1509–1518.
25 Y. Yoshida and T. Endo, *J. Polym. Sci., Part A:Polym. Chem.*, 2018, **56**, 2255–2262.
26 J. Zhang, F. Ye, J.-L. Huo, J.-W. Peng, R.-R. Hu and B. Z. Tang, *Chin. J. Polym. Sci.*, 2023, **41**, 1563–1576.
27 S. Watanabe, T. Takayama, H. Nishio, K. Matsushima, Y. Tanaka, S. Saito, Y. Sun and K. Oyaizu, *Polym. Chem.*, 2022, **13**, 1705–1711.
28 M. Fox, *Optical Properties of Solids*, OUP, Oxford, 2001, vol. 70.
29 S. Yoo, H. Park, Y. S. Kim, J. C. Won, D.-G. Kim and Y. H. Kim, *J. Mater. Chem. C*, 2021, **9**, 77–81.
30 K. Kikkawa, Y. Sumiya, K. Okazawa, K. Yoshizawa, Y. Itoh and T. Aida, *J. Am. Chem. Soc.*, 2024, **146**, 21168–21175.
31 Y. Fujisawa, Y. Nan, A. Asano, Y. Yanagisawa, K. Yano, Y. Itoh and T. Aida, *Angew. Chem., Int. Ed.*, 2023, **62**, e202214444.
32 A. Asano and T. Kurotu, *J. Mol. Struct.*, 1998, **441**, 129–135.
33 S. Watanabe, T. Takayama and K. Oyaizu, *ACS Polym. Au*, 2022, **2**, 458–466.
34 Y. Hu, L. Zhang, Z. Wang, R. Hu and B. Z. Tang, *Polym. Chem.*, 2023, **14**, 2617–2623.
35 J. W. Wu, R. W. Kulow, M. J. Redding, A. J. Fine, S. M. Grayson and Q. Michaudel, *ACS Polym. Au*, 2023, **3**, 259–266.